



Measurements of the charged particle multiplicity distribution in restricted rapidity intervals

D. Buskulic, D. Casper, I. de Bonis, D. Decamp, P. Ghez, C. Goy, J.P. Lees,
A. Lucotte, M.N. Minard, P. Odier, et al.

► To cite this version:

D. Buskulic, D. Casper, I. de Bonis, D. Decamp, P. Ghez, et al.. Measurements of the charged particle multiplicity distribution in restricted rapidity intervals. *Zeitschrift für Physik C Particles and Fields*, 1995, 69, pp.15-25. in2p3-00002085

HAL Id: in2p3-00002085

<https://hal.in2p3.fr/in2p3-00002085>

Submitted on 17 May 1999

HAL is a multi-disciplinary open access archive for the deposit and dissemination of scientific research documents, whether they are published or not. The documents may come from teaching and research institutions in France or abroad, or from public or private research centers.

L'archive ouverte pluridisciplinaire **HAL**, est destinée au dépôt et à la diffusion de documents scientifiques de niveau recherche, publiés ou non, émanant des établissements d'enseignement et de recherche français ou étrangers, des laboratoires publics ou privés.

Measurements of the Charged Particle Multiplicity Distribution in Restricted Rapidity Intervals

The ALEPH Collaboration ¹

Abstract

Charged particle multiplicity distributions have been measured with the ALEPH detector in restricted rapidity intervals $|Y| \leq 0.5, 1.0, 1.5, 2.0$ along the thrust axis and also without restriction on rapidity. The distribution for the full range can be parametrized by a log-normal distribution. For smaller windows one finds a more complicated structure, which is understood to arise from perturbative effects. The negative-binomial distribution fails to describe the data both with and without the restriction on rapidity. The JETSET model is found to describe all aspects of the data while the width predicted by HERWIG is in significant disagreement.

Submitted to Zeitschrift für Physik

¹See next pages for the list of authors

The ALEPH Collaboration

D. Buskalic, D. Casper, I. De Bonis, D. Decamp, P. Ghez, C. Goy, J.-P. Lees, A. Lucotte, M.-N. Minard, P. Odier, B. Pietrzyk

Laboratoire de Physique des Particules (LAPP), IN²P³-CNRS, 74019 Annecy-le-Vieux Cedex, France

F. Ariztizabal, M. Chmeissani, J.M. Crespo, I. Efthymiopoulos, E. Fernandez, M. Fernandez-Bosman, V. Gaitan, Ll. Garrido,¹⁵ M. Martinez, S. Orteu, A. Pacheco, C. Padilla, F. Palla, A. Pascual, J.A. Perlas, F. Sanchez, F. Teubert

Institut de Fisica d'Altes Energies, Universitat Autònoma de Barcelona, 08193 Bellaterra (Barcelona), Spain⁷

A. Colaleo, D. Creanza, M. de Palma, A. Farilla, G. Gelao, M. Girone, G. Iaselli, G. Maggi,³ M. Maggi, N. Marinelli, S. Natali, S. Nuzzo, A. Ranieri, G. Raso, F. Romano, F. Ruggieri, G. Selvaggi, L. Silvestris, P. Tempesta, G. Zito

Dipartimento di Fisica, INFN Sezione di Bari, 70126 Bari, Italy

X. Huang, J. Lin, Q. Ouyang, T. Wang, Y. Xie, R. Xu, S. Xue, J. Zhang, L. Zhang, W. Zhao

Institute of High-Energy Physics, Academia Sinica, Beijing, The People's Republic of China⁸

G. Bonvicini, M. Cattaneo, P. Comas, P. Coyle, H. Drevermann, A. Engelhardt, R.W. Forty, M. Frank, R. Hagelberg, J. Harvey, R. Jacobsen,²⁴ P. Janot, B. Jost, J. Knobloch, I. Lehraus, C. Markou,²³ E.B. Martin, P. Mato, H. Meinhard, A. Minten, R. Miquel, T. Oest, P. Palazzi, J.R. Pater,²⁷ J.-F. Pustaszneri, F. Ranjard, P. Rensing, L. Rolandi, D. Schlatter, M. Schmelling, O. Schneider, W. Tejessy, I.R. Tomalin, A. Venturi, H. Wachsmuth, W. Wiedenmann, T. Wildish, W. Witzeling, J. Wotschack

European Laboratory for Particle Physics (CERN), 1211 Geneva 23, Switzerland

Z. Ajaltouni, M. Bardadin-Otwinowska,² A. Barres, C. Boyer, A. Falvard, P. Gay, C. Guicheney, P. Henrard, J. Jousset, B. Michel, S. Monteil, J.-C. Montret, D. Pallin, P. Perret, F. Podlyski, J. Proriot, J.-M. Rossignol, F. Saadi

Laboratoire de Physique Corpusculaire, Université Blaise Pascal, IN²P³-CNRS, Clermont-Ferrand, 63177 Aubière, France

T. Fearnley, J.B. Hansen, J.D. Hansen, J.R. Hansen, P.H. Hansen, B.S. Nilsson

Niels Bohr Institute, 2100 Copenhagen, Denmark⁹

A. Kyriakis, E. Simopoulou, I. Siotis, A. Vayaki, K. Zachariadou

Nuclear Research Center Demokritos (NRCD), Athens, Greece

A. Blondel,²¹ G. Bonneaud, J.C. Brient, P. Bourdon, L. Passalacqua, A. Rougé, M. Rumpf, R. Tanaka, A. Valassi,³¹ M. Verderi, H. Videau

Laboratoire de Physique Nucléaire et des Hautes Energies, Ecole Polytechnique, IN²P³-CNRS, 91128 Palaiseau Cedex, France

D.J. Candlin, M.I. Parsons

Department of Physics, University of Edinburgh, Edinburgh EH9 3JZ, United Kingdom¹⁰

E. Focardi, G. Parrini

Dipartimento di Fisica, Università di Firenze, INFN Sezione di Firenze, 50125 Firenze, Italy

M. Corden, M. Delfino,¹² C. Georgiopoulos, D.E. Jaffe

Supercomputer Computations Research Institute, Florida State University, Tallahassee, FL 32306-4052, USA^{13,14}

A. Antonelli, G. Bencivenni, G. Bologna,⁴ F. Bossi, P. Campana, G. Capon, V. Chiarella, G. Felici, P. Laurelli, G. Mannocchi,⁵ F. Murtas, G.P. Murtas, M. Pepe-Altarelli

Laboratori Nazionali dell'INFN (LNF-INFN), 00044 Frascati, Italy

S.J. Dorris, A.W. Halley, I. ten Have,⁶ I.G. Knowles, J.G. Lynch, W.T. Morton, V. O'Shea, C. Raine, P. Reeves, J.M. Scarr, K. Smith, M.G. Smith, A.S. Thompson, F. Thomson, S. Thorn, R.M. Turnbull

Department of Physics and Astronomy, University of Glasgow, Glasgow G12 8QQ, United Kingdom¹⁰

U. Becker, O. Braun, C. Geweniger, G. Graefe, P. Hanke, V. Hepp, E.E. Kluge, A. Putzer, B. Rensch, M. Schmidt, J. Sommer, H. Stenzel, K. Tittel, S. Werner, M. Wunsch

Institut für Hochenergiephysik, Universität Heidelberg, 69120 Heidelberg, Fed. Rep. of Germany¹⁶

R. Beuselinck, D.M. Binnie, W. Cameron, D.J. Colling, P.J. Dornan, N. Konstantinidis, L. Moneta, A. Moutoussi, J. Nash, G. San Martin, J.K. Sedgbeer, A.M. Stacey

Department of Physics, Imperial College, London SW7 2BZ, United Kingdom¹⁰

G. Dissertori, P. Girtler, E. Kneringer, D. Kuhn, G. Rudolph

Institut für Experimentalphysik, Universität Innsbruck, 6020 Innsbruck, Austria¹⁸

C.K. Bowdery, T.J. Brodbeck, P. Colrain, G. Crawford, A.J. Finch, F. Foster, G. Hughes, T. Sloan, E.P. Whelan, M.I. Williams

Department of Physics, University of Lancaster, Lancaster LA1 4YB, United Kingdom¹⁰

A. Galla, A.M. Greene, K. Kleinknecht, G. Quast, J. Raab, B. Renk, H.-G. Sander, R. Wanke, C. Zeitnitz

Institut für Physik, Universität Mainz, 55099 Mainz, Fed. Rep. of Germany¹⁶

J.J. Aubert, A.M. Bencheikh, C. Benchouk, A. Bonissent,²¹ G. Bujosa, D. Calvet, J. Carr, C. Diaconu, F. Etienne, M. Thulasidas, D. Nicod, P. Payre, D. Rousseau, M. Talby

Centre de Physique des Particules, Faculté des Sciences de Luminy, IN²P³-CNRS, 13288 Marseille, France

I. Abt, R. Assmann, C. Bauer, W. Blum, D. Brown,²⁴ H. Dietl, F. Dydak,²¹ G. Ganis, C. Gotzhein, K. Jakobs, H. Kroha, G. Lütjens, G. Lutz, W. Männer, H.-G. Moser, R. Richter, A. Rosado-Schlosser, R. Settles, H. Seywerd, U. Stierlin,² R. St. Denis, G. Wolf

Max-Planck-Institut für Physik, Werner-Heisenberg-Institut, 80805 München, Fed. Rep. of Germany¹⁶

R. Alemany, J. Boucrot, O. Callot, A. Cordier, F. Courault, M. Davier, L. Duflot, J.-F. Grivaz, Ph. Heusse, M. Jacquet, D.W. Kim,¹⁹ F. Le Diberder, J. Lefrançois, A.-M. Lutz, G. Musolino, I. Nikolic, H.J. Park, I.C. Park, M.-H. Schune, S. Simion, J.-J. Veillet, I. Videau

Laboratoire de l'Accélérateur Linéaire, Université de Paris-Sud, IN²P³-CNRS, 91405 Orsay Cedex, France

D. Abbaneo, P. Azzurri, G. Bagliesi, G. Batignani, S. Bettarini, C. Bozzi, G. Calderini, M. Carpinelli, M.A. Ciocci, V. Ciulli, R. Dell'Orso, R. Fantechi, I. Ferrante, L. Foà,¹ F. Forti, A. Giassi, M.A. Giorgi, A. Gregorio, F. Ligabue, A. Lusiani, P.S. Marrocchesi, A. Messineo, G. Rizzo, G. Sanguinetti, A. Sciabà, P. Spagnolo, J. Steinberger, R. Tenchini, G. Tonelli,²⁶ G. Triggiani, C. Vannini, P.G. Verdini, J. Walsh

Dipartimento di Fisica dell'Università, INFN Sezione di Pisa, e Scuola Normale Superiore, 56010 Pisa, Italy

A.P. Betteridge, G.A. Blair, L.M. Bryant, F. Cerutti, Y. Gao, M.G. Green, D.L. Johnson, T. Medcalf, L.L.M. Mir, P. Perrodo, J.A. Strong

Department of Physics, Royal Holloway & Bedford New College, University of London, Surrey TW20 OEX, United Kingdom¹⁰

V. Bertin, D.R. Botterill, R.W. Clift, T.R. Edgecock, S. Haywood, M. Edwards, P. Maley, P.R. Norton, J.C. Thompson

Particle Physics Dept., Rutherford Appleton Laboratory, Chilton, Didcot, Oxon OX11 0QX, United Kingdom¹⁰

B. Bloch-Devaux, P. Colas, H. Duarte, S. Emery, W. Kozanecki, E. Lançon, M.C. Lemaire, E. Locci, B. Marx, P. Perez, J. Rander, J.-F. Renardy, A. Rosowsky, A. Roussarie, J.-P. Schuller, J. Schwindling, D. Si Mohand, A. Trabelsi, B. Vallage

CEA, DAPNIA/Service de Physique des Particules, CE-Saclay, 91191 Gif-sur-Yvette Cedex, France¹⁷

R.P. Johnson, H.Y. Kim, A.M. Litke, M.A. McNeil, G. Taylor

Institute for Particle Physics, University of California at Santa Cruz, Santa Cruz, CA 95064, USA²²

A. Beddall, C.N. Booth, R. Boswell, S. Cartwright, F. Combley, I. Dawson, A. Koksai, M. Letho, W.M. Newton, C. Rankin, L.F. Thompson

Department of Physics, University of Sheffield, Sheffield S3 7RH, United Kingdom¹⁰

A. Böhrer, S. Brandt, G. Cowan, E. Feigl, C. Grupen, G. Lutters, J. Minguet-Rodriguez, F. Rivera,²⁵ P. Saraiva, L. Smolik, F. Stephan

Fachbereich Physik, Universität Siegen, 57068 Siegen, Fed. Rep. of Germany¹⁶

M. Apollonio, L. Bosisio, R. Della Marina, G. Giannini, B. Gobbo, F. Ragusa²⁰

Dipartimento di Fisica, Università di Trieste e INFN Sezione di Trieste, 34127 Trieste, Italy

J. Rothberg, S. Wasserbaech

Experimental Elementary Particle Physics, University of Washington, WA 98195 Seattle, U.S.A.

S.R. Armstrong, L. Bellantoni,³⁰ P. Elmer, Z. Feng, D.P.S. Ferguson, Y.S. Gao, S. González, J. Grahl, J.L. Harton,²⁸ O.J. Hayes, H. Hu, P.A. McNamara III, J.M. Nachtman, W. Orejudos, Y.B. Pan, Y. Saadi, M. Schmitt, I.J. Scott, V. Sharma,²⁹ J.D. Turk, A.M. Walsh, Sau Lan Wu, X. Wu, J.M. Yamartino, M. Zheng, G. Zobernig

Department of Physics, University of Wisconsin, Madison, WI 53706, USA¹¹

¹Now at CERN, 1211 Geneva 23, Switzerland.

²Deceased.

³Now at Dipartimento di Fisica, Università di Lecce, 73100 Lecce, Italy.

⁴Also Istituto di Fisica Generale, Università di Torino, Torino, Italy.

⁵Also Istituto di Cosmo-Geofisica del C.N.R., Torino, Italy.

⁶Now at TSM Business School, Enschede, The Netherlands.

⁷Supported by CICYT, Spain.

⁸Supported by the National Science Foundation of China.

⁹Supported by the Danish Natural Science Research Council.

¹⁰Supported by the UK Particle Physics and Astronomy Research Council.

¹¹Supported by the US Department of Energy, contract DE-AC02-76ER00881.

¹²On leave from Universitat Autònoma de Barcelona, Barcelona, Spain.

¹³Supported by the US Department of Energy, contract DE-FG05-92ER40742.

¹⁴Supported by the US Department of Energy, contract DE-FC05-85ER250000.

¹⁵Permanent address: Universitat de Barcelona, 08208 Barcelona, Spain.

¹⁶Supported by the Bundesministerium für Forschung und Technologie, Fed. Rep. of Germany.

¹⁷Supported by the Direction des Sciences de la Matière, C.E.A.

¹⁸Supported by Fonds zur Förderung der wissenschaftlichen Forschung, Austria.

¹⁹Permanent address: Kangnung National University, Kangnung, Korea.

²⁰Now at Dipartimento di Fisica, Università di Milano, Milano, Italy.

²¹Also at CERN, 1211 Geneva 23, Switzerland.

²²Supported by the US Department of Energy, grant DE-FG03-92ER40689.

²³Now at University of Athens, 157-71 Athens, Greece.

²⁴Now at Lawrence Berkeley Laboratory, Berkeley, CA 94720, USA.

²⁵Partially supported by Colciencias, Colombia.

²⁶Also at Istituto di Matematica e Fisica, Università di Sassari, Sassari, Italy.

²⁷Now at Schuster Laboratory, University of Manchester, Manchester M13 9PL, UK.

²⁸Now at Colorado State University, Fort Collins, CO 80523, USA.

²⁹Now at University of California at San Diego, La Jolla, CA 92093, USA.

³⁰Now at Fermi National Accelerator Laboratory, Batavia, IL 60510, USA.

³¹Supported by the Commission of the European Communities, contract ERBCHBICT941234.

1 Introduction

A previous paper presented an analysis of the charged particle multiplicity distribution in hadronic Z decays [1]. In this paper the study is extended to restricted central rapidity intervals along the thrust axis. Energy-momentum and charge conservation strongly influence the multiplicity distribution for the full phase space. The distribution in restricted rapidity intervals, however, is less subject to such constraints and thus can be expected to be a more sensitive probe to the underlying dynamics of QCD.

The work presented here is based on a sample of 300,000 hadronic events at $\sqrt{s} = M_Z$ measured with the ALEPH detector at LEP in 1992, and 1,600,000 Monte Carlo events generated with the JETSET 7.3 parton shower model [2, 3] for detector corrections and investigation of systematic errors. The analysis was done in central rapidity intervals with $|Y| \leq 2.0$, which are essentially unaffected by charge conservation effects, as well as without restriction on rapidity.

The paper is organized as follows: section 2 contains a brief summary of the data analysis. The unfolding procedure used to correct the raw measurements for detector effects is reviewed briefly in section 3. Section 4 describes the model independent results obtained for the charged particle multiplicity distributions. A detailed study of parametric models is presented in section 5. Sections 6 and 7 summarize the results.

2 Data analysis

Details of the ALEPH detector and trigger system can be found in Reference [4]. For hadronic Z decays the trigger is practically 100% efficient. Here only a brief description of the detector components relevant for this analysis will be given. The momenta of charged tracks are measured with the ALEPH tracking system inside a 1.5 T magnetic field. The main component of this is a large time projection chamber (TPC) of radius of 1.8 m, which yields up to 21 space points per track. The single coordinate resolution of the TPC is typically 1.2 mm along z , defined by the beam direction, and $180 \mu\text{m}$ in $r\phi$, the transverse plane. Inside the TPC a conventional drift chamber (ITC) provides up to 8 additional coordinates per track, which are used in extrapolating the TPC tracks to a silicon vertex detector (VDET). A momentum resolution of $\Delta p/p^2 = 0.0006 (\text{GeV}/c)^{-1}$ is achieved by the combined system of TPC, ITC and VDET. Like-sign charged tracks with $p > 5 \text{ GeV}/c$ are fully resolved at opening angles greater than 2 degrees.

An event was accepted as hadronic if it had at least 5 charged tracks, a total charged energy in excess of 15 GeV, and if the polar angle of the sphericity axis with respect to the beam was in the range $35^\circ \leq \theta_{sph} \leq 145^\circ$. Each track was required to have at least 4 coordinates in the TPC and to originate from a cylindrical region with radius $d_0 = 3 \text{ cm}$ and length $z_0 = 5 \text{ cm}$ around the interaction point. The transverse momentum p_T with respect to the beam axis had to be larger than $200 \text{ MeV}/c$ and the polar angle between 20° and 160° .

The true charged multiplicity of an event was defined as the number of charged tracks that is obtained if all particles with a mean lifetime $\tau \leq 1 \text{ ns}$ decay while the others are stable. Thus, charged decay products of K_s^0 's and strange baryons are included. Apart from decay corrections, the measured charged multiplicity of an event can differ from that defined above because of acceptance losses or secondary interactions of particles with detector material. The data were corrected for $e^+e^- \rightarrow \tau^+\tau^-$ events, which contribute roughly 0.25% of the accepted events. This was found to be the only important background. The background is concentrated at low multiplicities and was subtracted bin-by-bin using a Monte Carlo simulation [5].

The relation between the observed multiplicity distribution $O_i(y)$ in a rapidity interval $|Y| \leq y$

and the underlying true distribution $T_j(y)$ can be described by a matrix equation,

$$O_i(y) = \sum_j G_{ij}(y) \cdot T_j(y) = \sum_j \tilde{G}_{ij}(y) \varepsilon_j(y) \cdot T_j(y) \quad . \quad (1)$$

The response matrix $G_{ij}(y)$ describes distortions due to detector effects and event selection. It is defined as the probability $\varepsilon_j(y)$ that an event with a true multiplicity j in the rapidity interval under consideration survives the event selection cuts, times the probability $\tilde{G}_{ij}(y)$ to observe i charged tracks instead of the true number j in the same interval. The matrices $G_{ij}(y)$ were determined from Monte Carlo simulations of a sample of 1.6M hadronic Z decays, generated with the JETSET parton shower model and processed by the full ALEPH detector simulation, reconstruction and analysis chain.

By construction the response matrices $G_{ij}(y)$ are independent of the relative frequencies with which events of a fixed true multiplicity j are produced by the Monte Carlo generator. Therefore they are only weakly dependent on the actual choice of the generator. Monte Carlo studies show that the measured multiplicities scatter around the respective true values with an rms-spread from approximately 1.8 to 3.7 units when the true multiplicity goes from $n_{true} = 8$ to $n_{true} = 30$. This smearing is almost independent of the size of the rapidity window under consideration. For clarity of notation the argument (y) specifying the rapidity interval will be omitted in the following where it is not explicitly needed.

By inverting Eq. (1) a model independent estimate for the true distributions T_j was extracted from the measurements. For this part of the analysis the raw response matrix obtained from the Monte Carlo was parametrized by a smooth function, because statistical fluctuations in the G_{ij} can create spurious structures in the corrected multiplicity distributions when solving Eq. (1) for T_j .

In a second analysis parametric models were studied. Here the true distribution $T_j = P_j(\vec{\Theta})$ is either given as a function of a vector of parameters $\vec{\Theta}$ or by the predictions from different Monte Carlo models. Given as input the respective true distributions T_j , the matrices G_{ij} were employed as convenient means to incorporate the effect of the full detector simulation. After multiplying T_j with the response matrix, the results were compared directly with the raw measurements. In case of the parametric models the parameters $\vec{\Theta}$ were determined by a standard least squares fit.

The multiplicity distributions were corrected for effects of initial state radiation (ISR) by applying bin-by-bin correction factors, determined from DYMU02 [6] plus the JETSET parton shower model. Except for the lowest multiplicity bins this correction turned out to be entirely negligible. In the model independent analysis the ISR corrections were applied to the unfolded distributions. For the parametric fits the effects of initial state radiation were included before folding with the response matrix.

3 The unfolding procedure

The relation between the true and the observed multiplicity distribution is stated formally by Eq. (1). Using it to infer the true distributions T_j from the measurements O_i implies “inverting” this equation, i.e. finding a distribution T_j which after folding with the response matrix G_{ij} as closely as possible matches the measurements O_i . Though seemingly trivial at first glance, this “unfolding” turns out to be a rather complicated problem in most cases.

The reason lies in the smearing effects parametrized by the response matrix. Events which have the same multiplicity at the level of the true distribution are spread over a finite range in the observed distribution. The width of this smearing tells how well individual events are measured and sets the scale for a bin width at which the measured distribution is essentially undistorted by

resolution effects. For low statistics this directly limits the number of bins that can be used, since for bin widths significantly smaller than the width of the smearing it is essentially impossible to disentangle to what extent neighboring bins of the true distribution contribute to adjacent bins of the observed distribution. Trying to correct for distortions by naively inverting Eq. (1) results in instabilities due to the statistical fluctuations in the measurements. A more in-depth analysis of the problem (see e.g. Ref. [7]) reveals that the loss of information due to resolution effects is so large that the naive inversion approach requires on the order of $N = \exp(n^2\sigma^2)$ events, where n is an effective number of bins of the unfolded distribution and σ the width of the response function in units of those bins. It follows that for the problem at hand unfolding methods are required for any realistically obtainable number of events.

Several ways of tackling the inverse problem Eq. (1) for finite statistics are discussed in the literature [8]. The basic idea always is to supplement the measurements by an additional constraint that stabilizes the unfolded result. In this analysis the “Method of reduced cross-entropy” (MRX) [9] was used in a first step to correct the measured distribution for smearing effects. In a second step the unfolded distribution was corrected for efficiency with bin-by-bin factors.

The MRX estimates an unfolded distribution $\tilde{T}_k = T_k \cdot \varepsilon_k$ by minimizing

$$F = w\chi^2 + S, \quad (2)$$

where

$$\chi^2 = \sum_{ij} \left(O_i - \sum_k \tilde{G}_{ik} \tilde{T}_k \right) (C^{-1})_{ij} \left(O_j - \sum_l \tilde{G}_{jl} \tilde{T}_l \right), \quad (3)$$

$$S = \sum_i P_i \ln \left(\frac{P_i}{\varepsilon_i} \right) \quad \text{with} \quad P_i = \tilde{T}_i / \sum_k \tilde{T}_k \quad (4)$$

and $w > 0$ is a weight factor which was adjusted according to the prescription in [9]. The covariance matrix C_{ij} of the measured distribution is diagonal for this analysis. The information about the measurements is contained in χ^2 . The stabilizing constraint is introduced by the function S which becomes minimal for $p_i = \varepsilon_i$, i.e. when the shape of the unsmeared distribution corresponds to a flat true distribution T_k . It is interesting to note that this criterion of “flatness” is formulated globally as a sum over all bins where the order of summation does not matter. No assumption about local curvature of the unfolded distribution is made. As a consequence, the regularization done by the inclusion of S , into the minimization corresponds to using the least restrictive assumption about the shape of the physical truth in a regularizing term. The constant w determines the relative weight of the measurements (χ^2) with respect to the smoothing term (S).

4 Model independent results

Tables 1 and 2 contain the model independent unfolded results for the charged particle multiplicity distributions of hadronic Z decays for the full phase space and rapidity intervals $|Y| \leq 0.5, 1.0, 1.5, 2.0$. The first error is statistical, the second one the systematic. Because of the unfolding procedure the errors are correlated. The data in Tab. 1 supersede the previously published results [1]. For the restricted rapidity intervals even and odd multiplicities are found; for the full Y-interval because of charge conservation only even values are allowed.

The unfolded distributions for the rapidity windows $|Y| \leq 0.5, 2.0$ and the full window are shown in Fig. 1. For comparison the predictions from the JETSET 7.3 [2] and the HERWIG 5.6 [10] parton shower models are overlayed together with the results from the parametric fits discussed

below. The parameters of the JETSET model have been tuned to distributions of global event shape variables and inclusive single particle spectra [3] as measured by ALEPH. For HERWIG an updated set of parameters is used following the procedure described in [3]. In going from small rapidity windows to the full phase space, not only the width of the multiplicity distribution grows steadily but also its shape changes significantly. It can be described by a simple curve whose second derivative is always negative for very small and very large intervals. For intermediate size intervals a pronounced shoulder structure develops. This kind of structure was first observed in proton-antiproton collisions [11] and points towards several independent components contributing to the charged particle multiplicity distribution. These are invisible for very small windows and average out when looking at the fully inclusive distribution covering the complete phase space. These independent components can be identified [12] with different event topologies, i.e. 2, 3 and 4-jet events, demonstrating that the charged particle multiplicity distribution carries information about the hard perturbative phase of multihadron production processes. A similar conclusion was obtained in a study of intermittency [13], where the multi-jet structure leads to bundles of particles with similar angles and hence similar rapidities relative to the thrust axis, resulting in large fluctuations in multiplicity at localized regions in rapidity.

The mean charged multiplicities $\langle n \rangle$ and the dispersion $D = \sqrt{\langle n^2 \rangle - \langle n \rangle^2}$ from the unfolded results compared to the model predictions are summarized in Table 3. The data are found to be in reasonable agreement with the JETSET prediction, whereas the HERWIG model exhibits significant discrepancies. The results for the full rapidity window are also in good agreement with the previously published values [1].

The systematic uncertainties given in the tables were estimated in the following way. Possible effects due to discrepancies between the actual and the simulated detector performance and the importance of background from $\tau^+\tau^-$ or two-photon events were studied by varying all track and event selection cuts described in section 2 one at a time and repeating the whole analysis for the modified set of cuts. For the track selection cuts the requirement of a minimum number of TPC hits was dropped and the p_T -cut was raised to 250 MeV/c, i.e. changed by an amount corresponding to the range over which the TPC becomes fully efficient. The d_0 and z_0 -cut were varied by ± 1 cm and ± 2 cm, respectively, and all angular cuts were varied by $\pm 5^\circ$. The minimum number of charged tracks required for the event was raised from 5 to 7 and the charged energy cut varied by ± 2.5 GeV. The resulting systematics are dominated by the change in the required number of TPC hits and the minimum transverse momentum of a track. The systematic uncertainty associated with the smoothing of the response matrix, or equivalently finite Monte Carlo statistics, was evaluated by including the difference between the nominal result and the result obtained with the non-smoothed matrix into the systematic errors. The residual generator dependence of the response matrix, which includes the extrapolation of the p_T -spectrum to $p_T = 0$, was taken to be the difference between the results found when using a response matrix determined with HERWIG instead of JETSET.

Furthermore, effects on the mean charged multiplicities due to the uncertainty in the rate of photon conversions, the reconstruction of decay products from V0's and the two-track resolution of the TPC were considered. Globally photon conversion rates are simulated correctly almost to the percent level; however, for some regions of the detector one finds discrepancies as large as 5%. With the number of conversions amounting roughly to 1 track/event, this corresponds to a systematic error of 0.05 tracks/event from this source. Recent measurements of V^0 production at ALEPH [14] gave systematic errors for K^0 and Λ production of 0.047 and 0.016 particles/event. Translating this to the number of charged tracks that should be visible, the systematic error on the mean charged particle multiplicity is 0.05 units. The effect of the finite two-track resolution of the TPC was taken from the previous analysis [1], which estimated this contribution to the systematic error to be 0.04 tracks/event.

Having evaluated the systematic uncertainties for the full phase space they were propagated to the mean multiplicities in each rapidity interval by rescaling them to the size of the interval. The errors on the mean value were then propagated into errors of the dispersion by assuming that they correspond to the mean of Poissonian fluctuations of particle pairs in case of the full rapidity window, and of individual particles for the restricted rapidity intervals. Folding the corrected distribution with the corresponding Poissonian, the errors on the mean value were thus translated to the individual bins and also into higher moments of the unfolded distributions. A breakdown of the individual contributions to the total systematic error of the mean value of the unfolded multiplicity distributions is given in Table 4.

5 Parametric models

Several parametrizations for the shape of the charged particle multiplicity distribution are discussed in the literature. Here we concentrate on two,

- the negative binomial distribution (NBD), and
- the log-normal distribution (LND).

The negative binomial distribution, first introduced as a parametrization for the multiplicity distribution by the UA5 Collaboration [15], is given by

$$P_n(< n >, k) = \frac{k(k+1)\dots(k+n-1)}{n!} \left(\frac{< n >}{< n > + k} \right)^n \left(1 + \frac{< n >}{k} \right)^{-k} . \quad (5)$$

Theoretically the NBD can be derived from the so-called clan model [16] for multiparticle production. Here an event consists on average of $N = k \ln(1 + < n > / k)$ clans which on average decay into $< n > / N$ secondary particles. In the context of QCD those clans might be identified with a number of N partons created in a parton-showering process that hadronize into $< n >$ final state particles. Perturbative QCD predicts, in fact, that the ratios of moments of the charged particle multiplicity distribution behave approximately like those of the NBD [17]. Experimentally the NBD was found to provide a good fit for a large number of charged particle multiplicity distributions measured at lower energies in a variety of reactions such as hadron-hadron or lepton-nucleon scattering [18] and e^+e^- -annihilation [19]. Good parametrizations were obtained both over the full and over restricted regions of phase space. Recent results at LEP energies [12], however, showed that the NBD fails to describe the data when studying multiplicity distributions in restricted rapidity intervals.

The LND can be derived from the general assumption that multi-particle production proceeds via a scale invariant stochastic branching process [20]. Here the final state multiplicity evolves over many generations, with the multiplicity ratio between successive generations described by independent random variables ε_i , $n_{i+1}/n_i = 1 + \varepsilon_i$. In the limit of a large number of branching processes the LND follows from the central limit theorem. From the continuous LND the discrete probability distribution for charged particle multiplicity n is defined by

$$P_n(\mu, \sigma, c) = \int_n^{n+\delta n} \frac{N}{n' + c} \exp \left(- \frac{[\ln(n' + c) - \mu]^2}{2\sigma^2} \right) dn', \quad (6)$$

where μ , σ and c are adjustable parameters and N is a normalization factor. The integration intervals are $\delta n = 1$ for restricted rapidity intervals where even and odd multiplicities contribute, and $\delta n = 2$ for the full phase space where charge conservation ensures that the total number of particles is always even. The LND gives a good fit to the charged particle multiplicity distributions

of e^+e^- -annihilation for the full phase space from low energy measurements up to LEP energies. This work extends the study of the LND to restricted rapidity intervals. Correlations between the parameters are reduced and a numerically stable fit of the LND is obtained by reexpressing σ^2 and μ as

$$\sigma^2 = \ln \left(1 + \frac{d^2}{(\bar{n} + c)^2} \right) \quad \text{and} \quad \mu = \ln \frac{(\bar{n} + c)^2}{\sqrt{d^2 + (\bar{n} + c)^2}}. \quad (7)$$

In the limit $\mu - \ln c \gg \sigma$ the new parameters \bar{n} and d can be identified as the mean and the standard deviation of the continuous distribution (6). The mean value $\langle n \rangle$ of the discrete distribution and \bar{n} are related via $\bar{n} \approx \langle n \rangle + (\delta n)/2$.

The parameters for both types of distributions were obtained from a least squares fit to the measurements by minimizing the function

$$\chi^2 = \sum_{ij} \left(O_i - \sum_k G_{ik} P_k(\vec{\Theta}) r_k \right) (C^{-1})_{ij} \left(O_j - \sum_l G_{jl} P_l(\vec{\Theta}) r_l \right), \quad (8)$$

with C_{ij} the covariance matrix of the measured distribution O_i in the corresponding rapidity interval and G_{ij} the raw response matrix. The coefficients r_k include the effect of initial state radiation into the model predictions. Since the model already is inherently smooth, no smoothing of the response matrix is required.

The fitted parameters for all rapidity intervals are given in Table 5 for the negative binomial distribution and in Table 6 for the log-normal distribution. Parameters and χ^2 -values in the rows labeled “stat” are for the nominal analysis with the covariance matrix describing only the statistical errors of the measurements. The first error denotes the statistical error of the parameters, the second one the systematic uncertainty, estimated in the usual way by varying the analysis as described before. Figure 1 also shows a comparison of the unfolded results with the parametric models.

The χ^2 of the fits was generally found to be rather large. In order to decide whether this apparent disagreement between model and data can be acomodated by systematic uncertainties, the fits with the nominal response matrix were re-done after including systematic errors into the covariance matrix of the measurements. This was done as follows, using the model independent unfolding results from the preceding section: For each variation of the selection cuts the unfolded distribution differs from the nominal result by a vector ΔP_j^{cut} . This vector, which is one contribution to the total systematic uncertainty of the unfolded distribution, was mapped onto a corresponding error vector in the space of the measurements by multiplying it with the response matrix:

$$\Delta O_i^{cut} = \sum_j G_{ij} \Delta P_j^{cut} \quad . \quad (9)$$

Using all vectors ΔO_i^{cut} corresponding to the systematic uncertainties discussed in section 2, a covariance matrix including statistical and systematic errors was defined via

$$\tilde{C}_{ij} = C_{ij} + \sum_{cuts} \Delta O_i^{cut} \Delta O_j^{cut} \quad . \quad (10)$$

Using the matrix \tilde{C}_{ij} instead of C_{ij} the fits were re-done. The results are given in Tables 5 and 6 in the rows labeled “full”. It is interesting to note that in those cases where the χ^2 was not too large when based on the statistical errors only, the central values of the parameters are stable within their systematic uncertainties. This is the case for fits of the LND. Looking at the χ^2 -values one sees that even after taking the systematic uncertainties into account, the parametric models in most cases fail to describe the data. The only exceptions are the log-normal distribution for very small rapidity windows $|Y| \leq 0.5$ or the full window.

6 Discussion of the Results

Figure 2 shows how the various estimates for the charged particle multiplicity distribution compare to the measurements in a narrow ($|Y| \leq 0.5$), a medium size ($|Y| \leq 2.0$) and the full rapidity window. In all cases the estimates for the true distribution, displayed in Fig. 1, were folded with the response matrix and then compared directly with the uncorrected data. The differences are shown in figure 2. For the unfolded data this constitutes a cross check of the procedure. For the four models the quality of the description of the data varies from being indistinguishable from the unfolded data to having a significant disagreement. The error bars reflect the statistical and systematic errors combined in quadrature; systematic uncertainties dominate.

The results clearly show that the NBD does not describe the data, either in restricted rapidity intervals or for the full phase space. The LND does fit the data for very small rapidity intervals, $|Y| \leq 0.5$, and the full window, but fails to do so for intermediate size intervals. Intuitively this can be understood from the fact that multi-jet effects mostly affect those medium size intervals, and it is not surprising that simple parametrizations like the LND or NBD fail when several components like two, three or multi-jet events contribute. In contrast to the simple parametric models both the JETSET and the HERWIG parton shower models reproduce the shoulder structure in the multiplicity distributions for intermediate size rapidity intervals. It is, however, interesting to note that of the two parton-shower models studied here only the JETSET model gives a good quantitative description of the charged particle multiplicity distribution in all rapidity intervals.

7 Summary and Conclusions

Charged particle multiplicity distributions for hadronic Z decays have been studied for various rapidity intervals along the thrust axis. A model independent unfolding of the measured distribution was done. The data were confronted with predictions from the JETSET and HERWIG Monte Carlo models and compared to analytical parametrizations given by a negative-binomial (NBD) and a log-normal distribution (LND).

The NBD consistently fails to describe the data. The LND provides a satisfactory parametrization for very small rapidity windows or for the full phase space. This supports the notion that both locally (small window) and globally (full phase space) multi-particle production can be understood as a scale invariant stochastic branching process. For intermediate size windows this simple picture is no longer valid because of hard gluon emission processes in the early stage of the perturbative cascade.

Hard gluon radiation as implemented in the JETSET and HERWIG Monte Carlo models at least qualitatively describes the shoulder structure of the multiplicity distribution in intermediate size rapidity intervals. Only JETSET, however, describes correctly also the details of the distribution. Studying the multiplicity distribution as function of the size of a rapidity window thus allows one to probe both hard and soft components of QCD.

Acknowledgements

We wish to thank our colleagues from the accelerator division for the successful operation of the LEP machine, and the engineers and technical staff in all our institutions for their contribution to the good performance of ALEPH. Those of us from non-member states thank CERN for its hospitality.

References

- [1] ALEPH Collaboration, D. Decamp et al., Phys. Lett. B 273 (1991) 181.
- [2] T. Sjöstrand, Comp. Phys. Comm. 27 (1982) 243;
T. Sjöstrand, Comp. Phys. Comm. 28 (1983) 229;
T. Sjöstrand and M. Bengtson, Comp. Phys. Comm. 43 (1987) 367.
- [3] ALEPH Collaboration, D. Buskulic et al., Z. Phys. C 55 (1992) 209.
- [4] ALEPH Collaboration, D. Decamp et al., Nucl. Instrum. and Methods A 294 (1990) 121.
- [5] S. Jadach, J.H. Kühn and Z. Was, Comp. Phys. Comm. 64 (1991) 275; S. Jadach, B.F.L. Ward and Z. Was, Comp. Phys. Comm. 66 (1991) 276.
- [6] J. E. Campagne and R. Zitoun, Z. Phys. C43 (1989) 469.
- [7] V. Blobel, DESY 84-118 (1984),
“Unfolding Methods in High Energy Physics Experiments”.
- [8] V.B. Anikeev and V.P. Zhigunov, Phys. Part. Nucl. 24 (4) 424, July-August 1993.
- [9] M. Schmelling, Nucl. Instrum. and Methods A 340 (1994) 400.
- [10] G. Marchesini and B.R. Webber, Nucl. Phys. B 310 (1988) 461;
G. Marchesini et al., Comp. Phys. Comm. 67 (1992) 465.
- [11] UA5 Collaboration, R.E. Ansorge et al., Z. Phys. C 43 (1989) 357.
- [12] DELPHI Collaboration, P. Abreu et al., Z. Phys. C 52 (1991) 511.
- [13] ALEPH Collaboration, D. Decamp et al., Z. Phys. C 53 (1992) 21.
- [14] ALEPH Collaboration, D. Buskulic et al., Z. Phys. C 64 (1994) 361.
- [15] UA5 Collaboration, G.J. Alner et al., Phys. Lett. B160 (1985) 193;
UA5 Collaboration, G.J. Alner et al., Phys. Lett. B160 (1985) 199;
UA5 Collaboration, G.J. Alner et al., Phys. Lett. B167 (1985) 476.
- [16] A. Giovannini and L. Van Hove, Z. Phys. C 30 (1986) 391.
- [17] E.D.Malaza and B.R. Webber, Phys. Lett. B149 (1984) 501;
E.D.Malaza and B.R. Webber, Nucl. Phys. B267 (1986) 702.
- [18] NA22 Collaboration, M. Adamus et al., Phys. Lett. B177 (1986) 239;
NA5 Collaboration, F. Dengler et al., Z. Phys. C33 (1986) 187;
WA25 Collaboration, B. Jongejans et al., Nuovo Cimento 101A (1989) 435;
EMC Collaboration, M. Arneodo et al., Z. Phys. C35 (1987) 335;
EHS-RCBC Collaboration, J. L. Bailly et al., Z. Phys. C40 (1988) 215;
SFM Collaboration, A. Breakstone et al., Nuovo Cimento 102A (1989) 1199.
- [19] HRS Collaboration, M. Derrick et al., Phys. Rev. D34 (1986) 3304;
TASSO Collaboration, W. Braunschweig et al., Z. Phys. C45 (1989) 193.
- [20] S. Carius and G. Ingelmann, Phys. Lett. B 252 (1990) 647;
R. Szwed and G. Wrochna, Z. Phys. C 47 (1990) 447;
R. Szwed, G. Wrochna and A.K. Wróblewski, Mod. Phys. Lett. A 5 (1990) 981.

n	P_n		
4	0.0020	\pm 0.0020	\pm 0.0027
6	0.0021	\pm 0.0009	\pm 0.0032
8	0.0058	\pm 0.0010	\pm 0.0023
10	0.0266	\pm 0.0018	\pm 0.0042
12	0.053	\pm 0.003	\pm 0.012
14	0.079	\pm 0.004	\pm 0.028
16	0.128	\pm 0.005	\pm 0.036
18	0.118	\pm 0.005	\pm 0.025
20	0.133	\pm 0.005	\pm 0.023
22	0.122	\pm 0.004	\pm 0.018
24	0.090	\pm 0.004	\pm 0.010
26	0.0760	\pm 0.0031	\pm 0.0064
28	0.0559	\pm 0.0029	\pm 0.0066
30	0.0389	\pm 0.0023	\pm 0.0032
32	0.0264	\pm 0.0018	\pm 0.0036
34	0.0166	\pm 0.0012	\pm 0.0039
36	0.0105	\pm 0.0010	\pm 0.0017
38	0.0080	\pm 0.0008	\pm 0.0024
40	0.0044	\pm 0.0006	\pm 0.0076
42	0.0019	\pm 0.0004	\pm 0.0017
44	0.0009	\pm 0.0002	\pm 0.0005
46	0.00076	\pm 0.00018	\pm 0.0010
48	0.00003	\pm 0.00004	\pm 0.0016
50	0.00038	\pm 0.00027	\pm 0.0005
52	0.00023	\pm 0.00009	\pm 0.0003
54	0.00013	\pm 0.00014	\pm 0.0002

Table 1: Unfolded charged particle multiplicity distribution giving the probability P_n to have a hadronic Z decay with n charged particles. The first error is the statistical error, the second the systematic uncertainty of the results. For $n=2$ no measurement was possible. The JETSET parton shower prediction is $P_2 = 0.000018 \pm 0.000004$.

n	P_n for $ Y \leq 0.5$			P_n for $ Y \leq 1.0$			P_n for $ Y \leq 1.5$			P_n for $ Y \leq 2.0$		
0	0.113	± 0.002	± 0.010	0.017	± 0.001	± 0.004	0.0033	± 0.0006	± 0.0008	0.0005	± 0.0005	± 0.0008
1	0.181	± 0.005	± 0.033	0.049	± 0.003	± 0.010	0.0115	± 0.0015	± 0.0031	0.0040	± 0.0008	± 0.0020
2	0.204	± 0.007	± 0.013	0.088	± 0.005	± 0.019	0.0245	± 0.0027	± 0.0052	0.0061	± 0.0013	± 0.0026
3	0.176	± 0.006	± 0.017	0.122	± 0.005	± 0.020	0.0585	± 0.0034	± 0.0076	0.018	± 0.002	± 0.013
4	0.102	± 0.004	± 0.015	0.126	± 0.004	± 0.011	0.0725	± 0.0034	± 0.0070	0.029	± 0.002	± 0.016
5	0.077	± 0.003	± 0.010	0.116	± 0.003	± 0.011	0.081	± 0.004	± 0.012	0.044	± 0.003	± 0.005
6	0.0525	± 0.0021	± 0.0063	0.097	± 0.003	± 0.005	0.096	± 0.004	± 0.012	0.059	± 0.003	± 0.018
7	0.0321	± 0.0019	± 0.0085	0.081	± 0.003	± 0.014	0.093	± 0.003	± 0.012	0.074	± 0.003	± 0.013
8	0.0217	± 0.0014	± 0.0035	0.064	± 0.002	± 0.011	0.0800	± 0.0031	± 0.0071	0.072	± 0.003	± 0.012
9	0.0136	± 0.0008	± 0.0032	0.0491	± 0.0019	± 0.0046	0.0658	± 0.0027	± 0.0068	0.067	± 0.002	± 0.004
10	0.0090	± 0.0006	± 0.0030	0.0373	± 0.0016	± 0.0061	0.0598	± 0.0021	± 0.0058	0.062	± 0.002	± 0.011
11	0.0066	± 0.0009	± 0.0023	0.0284	± 0.0013	± 0.0053	0.0533	± 0.0022	± 0.0057	0.0608	± 0.0023	± 0.0095
12	0.0034	± 0.0008	± 0.0033	0.0235	± 0.0013	± 0.0033	0.0451	± 0.0017	± 0.0044	0.0591	± 0.0020	± 0.0047
13	0.0035	± 0.0005	± 0.0021	0.0217	± 0.0013	± 0.0082	0.0371	± 0.0017	± 0.0047	0.0556	± 0.0022	± 0.0066
14	0.0023	± 0.0004	± 0.0015	0.0181	± 0.0010	± 0.0077	0.0315	± 0.0013	± 0.0038	0.0474	± 0.0019	± 0.0095
15	0.0017	± 0.0003	± 0.0018	0.0141	± 0.0009	± 0.0048	0.0274	± 0.0015	± 0.0041	0.0397	± 0.0017	± 0.0210
16	0.00072	± 0.00012	± 0.0006	0.0104	± 0.0006	± 0.0035	0.0245	± 0.0010	± 0.0024	0.0353	± 0.0015	± 0.0096
17	0.00040	± 0.00015	± 0.0005	0.0067	± 0.0007	± 0.0057	0.0221	± 0.0012	± 0.0054	0.0328	± 0.0015	± 0.0049
18	0.00028	± 0.00018	± 0.0004	0.0059	± 0.0005	± 0.0009	0.0187	± 0.0009	± 0.0035	0.0299	± 0.0013	± 0.0024
19	0.00004	± 0.00004	± 0.0002	0.0049	± 0.0004	± 0.0039	0.0159	± 0.0009	± 0.0033	0.0274	± 0.0014	± 0.0014
20				0.0044	± 0.0004	± 0.0007	0.0129	± 0.0008	± 0.0019	0.0250	± 0.0012	± 0.0068
21				0.0048	± 0.0007	± 0.0025	0.0113	± 0.0007	± 0.0009	0.0227	± 0.0012	± 0.0036
22				0.0029	± 0.0003	± 0.0022	0.0093	± 0.0007	± 0.0035	0.0197	± 0.0009	± 0.0020
23				0.0023	± 0.0004	± 0.0021	0.0081	± 0.0006	± 0.0013	0.0176	± 0.0010	± 0.0020
24				0.0016	± 0.0003	± 0.0013	0.0067	± 0.0004	± 0.0010	0.0144	± 0.0008	± 0.0071
25				0.0012	± 0.0002	± 0.0011	0.0054	± 0.0005	± 0.0011	0.0123	± 0.0008	± 0.0016
26				0.0008	± 0.0001	± 0.0007	0.0048	± 0.0006	± 0.0026	0.0104	± 0.0006	± 0.0013
27				0.0006	± 0.0001	± 0.0023	0.0039	± 0.0003	± 0.0013	0.0091	± 0.0006	± 0.0025
28				0.0004	± 0.0001	± 0.0004	0.0032	± 0.0004	± 0.0007	0.0081	± 0.0005	± 0.0018
29				0.0004	± 0.0001	± 0.0005	0.0027	± 0.0004	± 0.0012	0.0071	± 0.0006	± 0.0012
30				0.0002	± 0.0001	± 0.0003	0.0025	± 0.0004	± 0.0008	0.0059	± 0.0004	± 0.0019
31				0.0003	± 0.0001	± 0.0005	0.0020	± 0.0002	± 0.0006	0.0045	± 0.0004	± 0.0013
32				0.0003	± 0.0001	± 0.0005	0.0018	± 0.0002	± 0.0011	0.0037	± 0.0003	± 0.0012
33				0.0002	± 0.0003	± 0.0005	0.0012	± 0.0003	± 0.0011	0.00322	± 0.00033	± 0.0009
34							0.00097	± 0.00015	± 0.0004	0.00234	± 0.00035	± 0.0007
35							0.00072	± 0.00015	± 0.0004	0.00217	± 0.00021	± 0.0005
36							0.00035	± 0.00010	± 0.0003	0.00158	± 0.00020	± 0.0008
37							0.00009	± 0.00006	± 0.0002	0.00131	± 0.00012	± 0.0007
38							0.00013	± 0.00013	± 0.0003	0.00110	± 0.00017	± 0.0010
39							0.00003	± 0.00003	± 0.0005	0.00076	± 0.00012	± 0.0006
40										0.00052	± 0.00013	± 0.0007
41										0.00010	± 0.00006	± 0.0006
42										0.00073	± 0.00035	± 0.0010
43										0.00018	± 0.00007	± 0.0005
44										0.00022	± 0.00019	± 0.0005
45										0.00021	± 0.00015	± 0.0007

Table 2: Unfolded multiplicity distributions for restricted rapidity bins along the thrust axis. The first error is the statistical, the second the systematic error of the result. Note that because of the unfolding procedure neighboring bins are correlated over a range from approximately 2.6 units for $|Y| \leq 0.5$ to 3.6 units in multiplicity for the full phase space. In addition systematic effects, e.g. p_T -cuts, create correlations over longer ranges.

		$\langle n \rangle$	D	χ^2 per bin
$ Y \leq 0.5$	Unfolded result	$3.074 \pm 0.006 \pm 0.040$	$2.582 \pm 0.008 \pm 0.040$	0.85
	JETSET	3.038 ± 0.003	2.597 ± 0.003	1.57
	HERWIG	3.075 ± 0.003	2.721 ± 0.003	6.17
$ Y \leq 1.0$	Unfolded result	$6.436 \pm 0.009 \pm 0.081$	$4.54 \pm 0.01 \pm 0.15$	0.68
	JETSET	6.396 ± 0.005	4.588 ± 0.005	1.74
	HERWIG	6.384 ± 0.005	4.771 ± 0.005	6.65
$ Y \leq 1.5$	Unfolded result	$9.78 \pm 0.01 \pm 0.10$	$6.082 \pm 0.013 \pm 0.092$	0.90
	JETSET	9.797 ± 0.006	6.112 ± 0.006	1.64
	HERWIG	9.706 ± 0.006	6.348 ± 0.006	3.98
$ Y \leq 2.0$	Unfolded result	$13.01 \pm 0.01 \pm 0.12$	$7.068 \pm 0.013 \pm 0.089$	0.70
	JETSET	13.083 ± 0.007	7.026 ± 0.006	1.47
	HERWIG	12.925 ± 0.007	7.359 ± 0.006	8.43
full Y	Unfolded result	$20.91 \pm 0.03 \pm 0.22$	$6.425 \pm 0.031 \pm 0.087$	1.11
	JETSET	20.861 ± 0.006	6.298 ± 0.005	1.38
	HERWIG	20.695 ± 0.007	6.976 ± 0.006	34.4

Table 3: Unfolded mean charged multiplicity $\langle n \rangle$ and dispersion D compared to expectations from the JETSET and HERWIG models.

Source	$ Y \leq 0.5$	$ Y \leq 1.0$	$ Y \leq 1.5$	$ Y \leq 2.0$	full Y
Generator dependence	0.015	0.034	0.020	0.027	0.09
Monte Carlo statistics	0.005	0.004	0.003	0.006	0.02
Number of TPC hits	0.031	0.058	0.081	0.094	0.12
p_T cut	0.014	0.036	0.046	0.057	0.06
other cut variations	0.006	0.010	0.021	0.029	0.12
2-track resolution	0.006	0.012	0.019	0.025	0.04
γ conversions	0.007	0.015	0.023	0.031	0.05
V^0 's	0.007	0.015	0.023	0.031	0.05
total	0.040	0.081	0.10	0.12	0.22

Table 4: Breakdown of the systematic errors of the unfolded mean charged multiplicity $\langle n \rangle$.

	errors	\bar{n}	k	χ^2 / ndf
$ Y \leq 0.5$	stat.	$3.050 \pm 0.006 \pm 0.040$	$2.84 \pm 0.03 \pm 0.017$	596 / 19
	full	3.292	2.46	272 / 19
$ Y \leq 1.0$	stat.	$6.366 \pm 0.010 \pm 0.085$	$3.32 \pm 0.02 \pm 0.021$	2883 / 31
	full	5.507	5.01	906 / 31
$ Y \leq 1.5$	stat.	$9.74 \pm 0.01 \pm 0.12$	$3.86 \pm 0.02 \pm 0.14$	3906 / 41
	full	10.40	3.29	1155 / 41
$ Y \leq 2.0$	stat.	$13.02 \pm 0.01 \pm 0.16$	$4.78 \pm 0.02 \pm 0.12$	2627 / 44
	full	12.05	4.67	780 / 44
full Y	stat.	$20.91 \pm 0.01 \pm 0.17$	$22.73 \pm 0.17 \pm 0.85$	654 / 43
	full	21.01	22.00	160 / 43

Table 5: Results from fitting negative-binomial distributions.

	errors	μ	d	c	χ^2 / ndf
$ Y \leq 0.5$	stat.	$3.506 \pm 0.008 \pm 0.043$	$2.609 \pm 0.008 \pm 0.043$	$1.64 \pm 0.06 \pm 0.014$	80.7 / 18
	full	3.548	2.660	1.34	21.7 / 18
$ Y \leq 1.0$	stat.	$6.911 \pm 0.009 \pm 0.092$	$4.55 \pm 0.01 \pm 0.22$	$1.45 \pm 0.04 \pm 0.34$	449 / 30
	full	6.712	4.37	1.35	138 / 30
$ Y \leq 1.5$	stat.	$10.24 \pm 0.01 \pm 0.20$	$6.12 \pm 0.01 \pm 0.55$	$1.88 \pm 0.06 \pm 0.96$	1170 / 40
	full	10.12	6.07	1.89	563 / 40
$ Y \leq 2.0$	stat.	$13.47 \pm 0.01 \pm 0.24$	$7.13 \pm 0.01 \pm 0.47$	$3.5 \pm 0.1 \pm 1.7$	1614 / 43
	full	13.08	6.98	3.9	570 / 43
full Y	stat.	$21.94 \pm 0.01 \pm 0.17$	$6.373 \pm 0.012 \pm 0.059$	$7.5 \pm 0.3 \pm 2.4$	75.8 / 42
	full	21.92	6.344	6.6	51.9 / 42

Table 6: Results from fitting log-normal distributions.

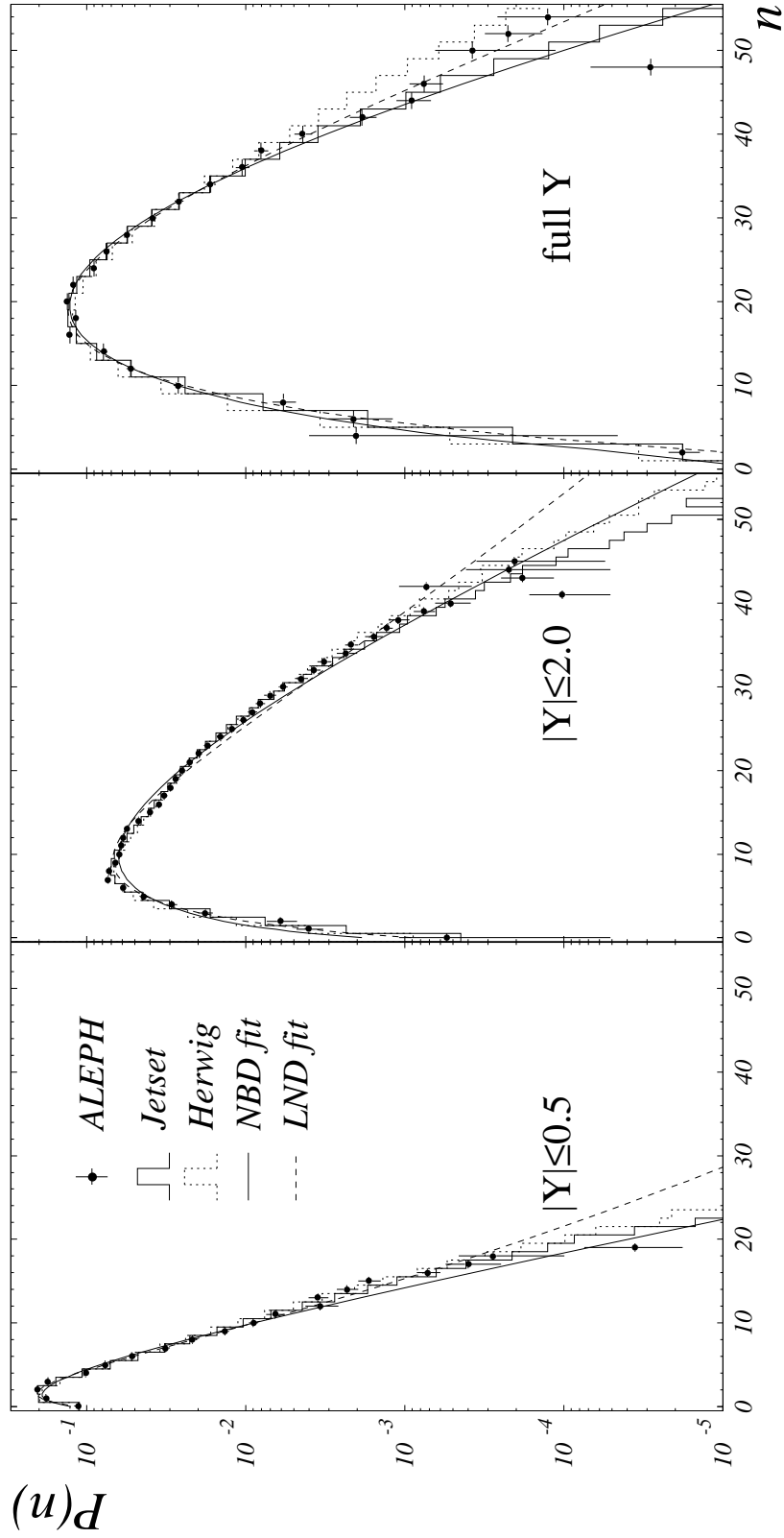


Figure 1: Unfolded charged particle multiplicity distributions for small ($|Y| \leq 0.5$, left), medium ($|Y| \leq 2.0$, middle) and the full rapidity window (right), compared to various models.

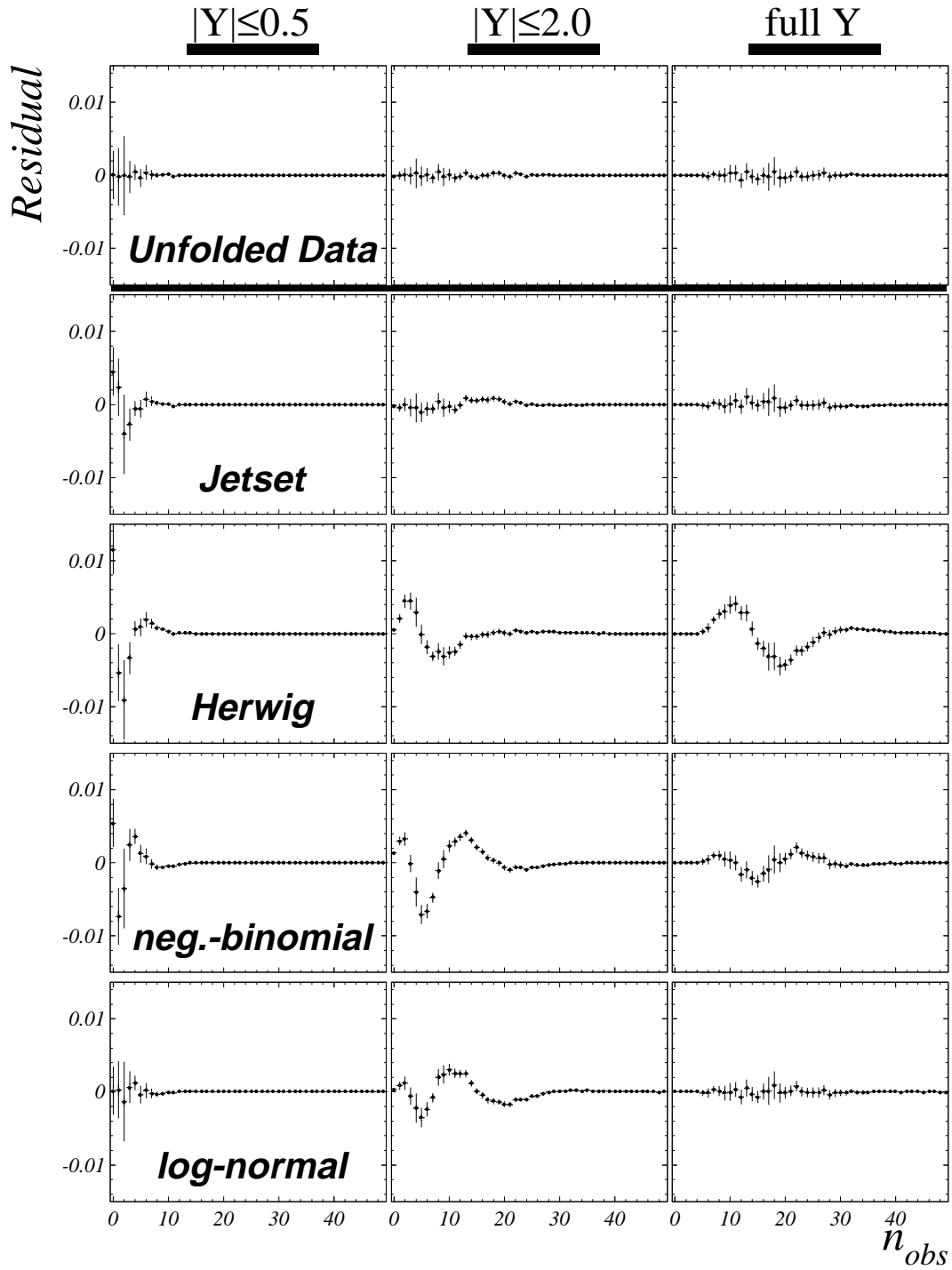


Figure 2: Comparison of raw data with unfolded results and various model predictions after convolution with the response matrix. The unfolded data are shown first as a consistency check of the unfolding procedure. The remaining plots display the differences between the data and the four models. Results are given for small ($|Y| \leq 0.5$, left), medium ($|Y| \leq 2.0$, middle) and the full rapidity window (right). The error bars reflect the statistical and systematic errors combined in quadrature; systematic uncertainties dominate.